Supplementary Information for

Freestanding 3D nanoporous Cu@1D Cu_2O nanowire heterostructure: From facile one-step protocol to robust application in Li storage

Wenbo Liu,[a,d,*] Long Chen,[a] Liu Cui,[b,d] Jiazhen Yan,[a] Shichao Zhang,[c] Sanqiang Shi[d]

[a] School of Manufacturing Science and Engineering, Sichuan University, Chengdu 610065, China

[b] Key Laboratory of Condition Monitoring and Control for Power Plant Equipment, Ministry of Education, North China Electric Power University, Beijing 102206, China

[c] School of Materials Science and Engineering, Beihang University, Beijing 100191, China

[d] Department of Mechanical Engineering, The Hong Kong Polytechnic University, Hung Hom, Kowloon, Hong Kong

Tel: +86-028-85405320; Fax: +86-028-85403408; E-mail: liuwenbo_8338@163.com.

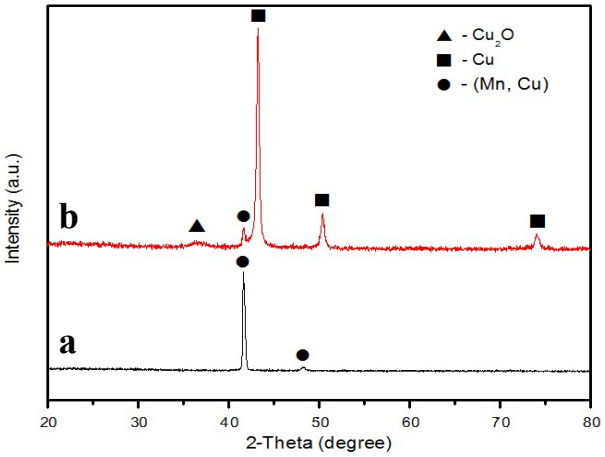

Figure S1. XRD patterns of as-cast Mn 35 at.% Cu alloy sheets (a) before and (b) upon electrochemical dealloying in the 5 wt.% H_2SO_4 solution at the potential of -0.2 V(SCE) for 60 min.

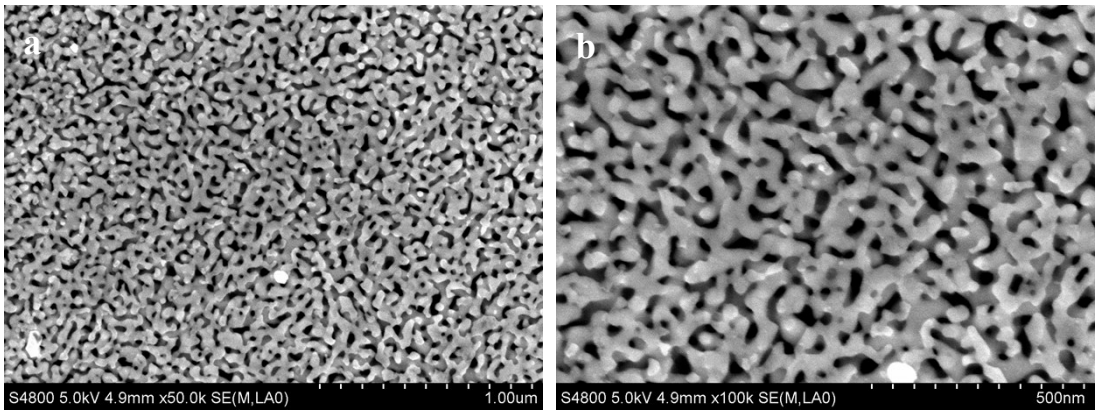

Figure S2. SEM images showing the microstructure of NPC by chemical dealloying of the as-cast Mn 35 at.% Cu alloy in the 5 wt.% H_2SO_4 solution for 24 h. Part b is the corresponding high-magnification image.

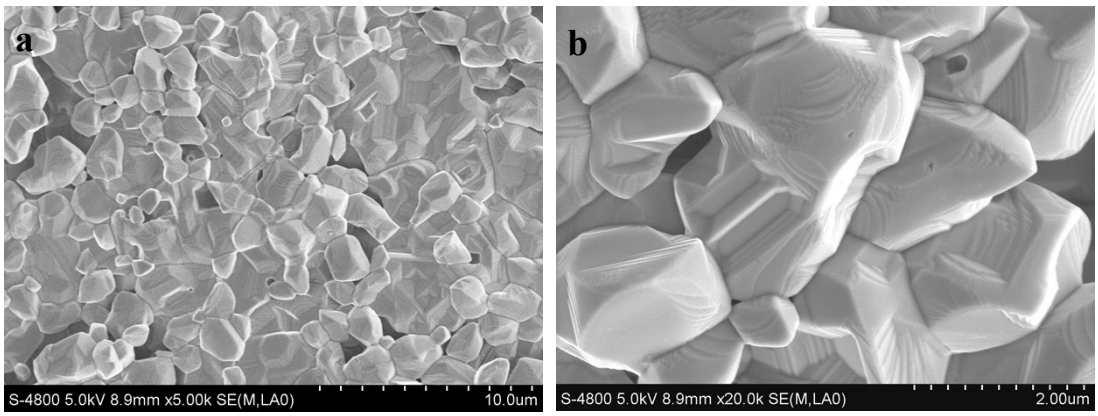

Figure S3. SEM images showing the microstructure of 2D PC@Cu_2O MPs electrode by two-step heat treatments of 2D planar copper at 550℃ for 1 h under ambient atmosphere following at 700℃ for 2 h under Ar atmosphere. Part b is the corresponding high-magnification image.

Supplementary Note 1

In Figure 5e-h, we present the original models and normalized von Mises stress distributions after Li^+ insertion of the NWNs and MPs electrodes by molecular dynamics (MD) simulation. The dimensions of the shown MD simulation domains are $14\times14\times24$ nm^3 and $22\times22\times22$ μm^3 for NWNs and MPs, respectively. Each domain contains 6 NWs/MPs. The diameter and length of Cu_2O NWs are 2 and 22 nm, respectively. The diameter of Cu_2O MPs is set as 10 μm. Correspondingly, the densities of simulation domains of Cu_2O NWNs and Cu_2O MPs are 0.6 and 2.1 g/cm^3. The construction of Li_2O takes into account the constant number of atoms of each element before and after Li^+ insertion reaction. Herein, the LAMMPS package is employed to carry out MD simulations.[1] The third-generation charge optimized many-body (COMB3) potential[2] is used to model interatomic interactions in Cu_2O NWNs/MPs. The FIT-EMP potential form,[3-4] which is one of Buckingham-type pairwise potential models, is adopted to describe the interatomic interactions in Li_2O NWNs/MPs. The van der Waals interactions are described by the Lennard-Jones (LJ) potential.[5] Periodic boundary conditions were applied in all directions. The time step is set as 0.5 fs. Starting from pre-optimized geometries, after initial equilibration in NVT ensemble, the systems are run in the NVE ensemble for 5 ns, from which the atomic stresses are extracted and post-processed.

The von Mises stress is introduced to estimate the stress distribution in systems. The von Mises stress (σ_M) for each atom can be calculated as:[6]

$$\sigma_{\mathrm{M}} = \sqrt{\left(\sigma_x - \sigma_y\right)^2 + \left(\sigma_y - \sigma_z\right)^2 + \left(\sigma_z - \sigma_x\right)^2 + 6(\tau_{xy} + \tau_{yz} + \tau_{xz})^2} \quad (1)$$

Where σ_{x}, σ_{y} and σ_{z} are the normal stresses along the three directions, and τ_{xy}, τ_{yz} and τ_{xz} are the shear stresses in three planes, respectively. As can be seen explicitly from Figure 5e-h, the NWs were just subjected to slightly large stress in the outmost layer (relative to low one in the interior), while the markedly greater stress can be found throughout the whole MPs (from outside to inside), clearly manifesting the relatively large stress concentration existing in the MPs. Besides, compared to the indistinguishable mussy structure of MPs after Li^+ insertion reaction, it is still so easy to discern six independent NWs, fully indicative of its good structure integrity and stability. As a result, the relatively large stress concentration and poor structure integrity can be identified in the MPs electrode after Li^+ insertion, which would be undoubtedly easier to cause the failure of electrode in comparison with the NWNs.

Table S1. Chemical compositions of the initial Mn-Cu alloy sheets by EDX analysis.

Precursor	Elements (at.%)	
	Mn	Cu
Initial Mn-Cu alloy	64.78	35.22

Table S2. A detailed comparison of Li storage properties of various Cu-based oxides and their nanocomposites with different structure designs.

Materials	Structure	Capacity	Cycles	Capacity retention	Ref.
NF/CuO*	nanorod	0.72 mAh cm^{-2}	150	38 %	7
3DGN/CuO*	composite	0.39 mAh cm^{-2}	50	71 %	8
Cu_xO/Cu	massif-like	1.8 mAh cm^{-2}	100	30 %	9
CNT-Cu_2O*	hybrid	0.23 mAh cm^{-2}	15	60 %	10
SnO/Cu_3Sn/Cu_2O/Cu	composite	7.4 mAh cm^{-2}	20	67 %	11
Cu@Cu_2O	nanoporous	1.45 mAh cm^{-2}	120	61 %	12
Cu_2O-Cu	nanoparticle	0.76 mAh cm^{-2}	100	36 %	13
CuO	nanowire	0.75 mAh cm^{-2}	120	80 %	14
Cu_2O/Cu	nanopillar	0.06 mAh cm^{-2}	20	50 %	15
Cu_2O/Cu	nanopillar	0.13 mAh cm^{-2}	50	73 %	16
$CuFe_2O_4$	nanoparticle	0.14 mAh cm^{-2}	3	68 %	17
Cu_2O	nanoparticle	350 mAh g^{-1}	100	58.3 %	18
CuO	hollow sphere	91 mAh g^{-1}	50	16.5 %	19
Cu_2O	porous film	213 mAh g^{-1}	50	63.4 %	20
CuO/Cu_2O	hollow polyhedron	440 mAh g^{-1}	100	58.6 %	21
CuO	nanohexagon	575 mAh g^{-1}	100	57.1 %	22
Cu_2O	nanorod array	358 mAh g^{-1}	200	33 %	23
Cu_2O/Cu	nanorod array	385 mAh g^{-1}	100	36 %	24
CuO/Cu_2O/Cu	cypress-like	534 mAh g^{-1}	100	52 %	25
CuO-Cu_2O/G*	nanosphere	487 mAh g^{-1}	60	46 %	26
Cu_2O/Cu	core-shell	360 mAh g^{-1}	50	52 %	27
Cu_2O/rGO*	octahedron	348 mAh g^{-1}	50	45 %	28
3D NPC@1D Cu_2O NWNs	1D/3D nano heterostructure	1.63 mAh cm^{-2} (≈627 mAh g^{-1})	150	60.2 %	Our work

* NF: Ni foam; 3DGN: 3D graphene network; CNT: Carbon nanotube; G: Graphene; rGO: Reduced graphene oxide.

Supplementary References

1 S. Plimpton, *J. Comput. Phys.*, 1995, **117**, 1-19.

2 T. Liang, T. R. Shan, Y. Cheng, B. D. Devine, M. Noordhoek, Y. Li, Z. Lu, S. R. Phillpot and S. B. Sinnott, *Mat. Sci. Eng. R*, 2013, **74**, 255-279.

3 R. A. Buckingham, *Proc. R. Soc. Lond. A*, 1938, **168**, 264-283.

4 T. Oda, Y. Oya, S. Tanaka and W. J. Weber, *J. Nucl. Mater.*, 2007, **367**, 263-268.

5 J. E. Jones, *Proc. R. Soc. Lond. A*, 1924, **106**, 463-477.

6 C. Wang, Y. Liu, L. Li and H. Tan, *Nanoscale*, 2014, **6**, 5703-5707.

7 C. M. Tang, H. Y. Zhang, D. L. Jiao, R. Z. Hu and Z. W. Liu, *Mater. Design*, 2019, **162**, 52-59.

8 D. Ji, H., Zhou, Y. Tong, J. Wang, M. Zhu, T. Chen and A. Yuan, *Chem. Eng. J.*, 2016, **313**, 1623-1632.

9 S. Ni, X. Lv, T. Li, X. Yang, L. Zhang and Y. Ren, *Electrochim. Acta*, 2013, **96**, 253-260.

10 A. Goyal, A. L. M. Reddy and P. M. Ajayan, *Small*, 2011, **7**, 1709-1713.

11 G. Han, J. H. Um, H. Park, K. Hong, W. S. Yoon and H. Choe, *Scripta Mater.*, 2018, **163**, 9-13.

12 D. Q. Liu, Z. B. Yang, P. Wang, F. Li, D. S. Wang and D. Y. He, *Nanoscale*, 2013, 5, 1917-1921.

13 S. Ni, X. Lv, T. Li, X. Yang and L. Zhang, *Electrochim. Acta*, 2013, **109**, 419-425.

14 R. Zhang, J. Liu, H. Guo and X. Tong, *Mater. Lett.*, 2015, **139**, 55-58.

15 B. Sun, H. D. Asfaw, D. Rehnlund, J. Mindemark, L. Nyholm, K. Edstrom and D. Brandell, *ACS Appl. Mater. Inter.*, 2018, **10**, 2407-2413.

16 M. Valvo, D. Rehnlund, U. Lafont, M. Hahlin, K. Edstrom and L. Nyholm, *J. Mater. Chem. A*, 2014, **2**, 9574-9586.

17 H. Zhao, H. Jia, S. Wang D. Xue and Z. Zheng, *J. Exp. Nanosci.*, 2011, **6**, 75-83.

18 P. Poizot, S. Laruelle, S. Grugeon, L. Dupont and J. M. Tarascon, *Nature*, 2000, **407**, 496-499.

19 J. C. Park, J. Kim, H. Kwon and H. Song, *Adv. Mater.*, 2009, **21**, 803-807.

20 J. Y. Xiang, X. L. Wang, X. H. Xia, L. Zhang, Y. Zhou, S. J. Shi and J. P. Tu, *Electrochim. Acta*, 2010, **55**, 4921-4925.

21 L. Hu, Y. M. Huang, F. P. Zhang and Q. W. Chen, *Nanoscale*, 2013, **5**, 4186-4190.

22 P. Subalakshmi and A. Sivashanmugam, *J. Alloys Compd.*, 2017, **690**, 523-531.

23 Y. M. Zhang, K. Wang, Z. H. Yang, Y. M. Zhang, H. Y. Gu, W. X. Zhang, E. R. Li and C. Zhou, *Thin Solid Films*, 2016, **608**, 79-87.

24 W. Q. Chen, W. F. Zhang, L. Chen, L. X. Zeng and M. D. Wei, *J. Alloys Compd*., 2017, **723**, 172-178.

25 S. Liu, H. Hou, X. Liu, J. Duan, Y. Yao and Q. Liao, *Ionics*, 2017, **23**, 1075-1082.

26 X. Zhou, J. Shi, Y. Liu, Q. Su, J. Zhang and G. Du, *J. Alloys Compd*., 2014, **615**, 390-394.

27 J. Y. Xiang, J. P. Tu, Y. F. Yuan, X. H. Huang, Y. Zhou and L. Zhang, *Electrochem. Commun.*, 2009, **11**, 262-265.

28 G. C. Yan, X. H. Li, Z. X. Wang, H. J. Guo, Q. Zhang and W. J. Peng, *T. Nonferr.*

Metal Soc., 2013, **23**, 3691-3696.